Comparison of CFD Modelling with Small-Scale Field Experiments of Chlorine Dispersion*

M. KIŠA, Ľ. JELEMENSKÝ**, O. MIERKA, and J. STOPKA

Department of Chemical and Biochemical Engineering, Faculty of Chemical and Food Technology, Slovak University of Technology, SK-812 37 Bratislava
e-mail: ludovit.jelemensky@stuba.sk

Received 1 April 2004

Dedicated to the 80th birthday of Professor Elemír Kossaczký

Nowadays, for safety purposes and due to the hazard assessment of industrial processes it is necessary to have a good tool for modelling gas dispersion. CFD modelling has the potential to be an important tool for more reliable prediction of concentration of dangerous species accidentally released into the atmosphere. Thus, also gas dispersion in complex-geometry environments can be solved. Parameters of such model, particularly the turbulent Schmidt number and the surface roughness length as well as their influence on the CFD modelling of gas (Cl_2) dispersion, were examined. The results were compared with the experimental data for a small release of chlorine gas.

The comparison revealed that the value of turbulent Schmidt number has an essential influence on the concentration prediction reliability and should be much lower compared to the values used in literature in the case of the atmospheric boundary layer. Moreover, it was found that the surface roughness plays a significant role for a realistic prediction of the contaminant concentration.

Dangerous materials, particularly toxic or flammable gases are often used in industry. Production, storing or piping of such material can lead to accidental releases of dangerous gases. Therefore, there is a need for a tool to predict pollutant concentrations in specific places in the vicinity of damaged apparatus or pipeline. Mathematical modelling can solve this problem, but first, these models must be specified and validated. These models are based on equations of mass, momentum, and energy balance for chosen space geometry. Actually, CFD modelling is more appropriate than the simpler models (Gauss model, box models, K-theory models, *etc.*) [1], as it is able to solve the balance equations for any possible geometric situation. However, it should be noted that the confidence of CFD simulation of fluid and mass dispersion, even for a simple geometry, must be checked with experimental results.

Therefore, this paper is focused on modelling of a continuous release of gas (chlorine) into the atmosphere. A simple geometry of open country with flat land was chosen. The main objective of the paper is to validate the CFD models against experimental observations [2] in order to provide further insight into the abilities of CFD models used to predict fluid flow and mass transport of dangerous substances in the atmosphere. The study was oriented on validation of some parameters of the CFD models used, particularly the roughness of the land and the most important parameter used in the diffusion equation, the turbulent Schmidt number. In this context the turbulent k-ε model was used.

THEORETICAL

Governing Equations for the Fluid Flow

Since in the atmospheric boundary layer turbulent fluid flow was assumed a turbulence model approach was employed. The governing equations of such a flow are equations of mass balance, momentum balance, and energy balance. However, in the present study the model was simplified by introducing isothermal flow. This assumption is valid when modelling was performed in 10 m above the ground.

The incompressible airflow in the atmospheric boundary layer may be mathematically described us-

*Presented at the 31st International Conference of the Slovak Society of Chemical Engineering, Tatranské Matliare, 24—28 May 2004.

**The author to whom the correspondence should be addressed.

ing the following Navier—Stokes equations, see [3]

$$\frac{\partial \rho}{\partial t} + \frac{\partial}{\partial x_j}(\rho u_j) = 0 \tag{1}$$

$$\frac{\partial}{\partial t}(\rho u_i) + \frac{\partial}{\partial x_j}(\rho u_i u_j) = \\ = -\frac{\partial p}{\partial x_i} + \frac{\partial}{\partial x_j}\left[\mu\left(\frac{\partial u_i}{\partial x_j} + \frac{\partial u_j}{\partial x_i}\right)\right] + \\ + \frac{\partial}{\partial x_j}\left(-\rho\overline{u_i' u_j'}\right) + \rho g \tag{2}$$

where the subscripts i, $j = 1, 2, 3$ refer to the components in the x, y, z of the Cartesian coordinate system, u is the velocity, p the pressure, ρ the density, μ the viscosity, g the gravitational constant, and u' the fluctuation velocity. The product of fluctuation velocities is the Reynolds stress tensor, which can be modelled by the Boussinesq hypothesis [4] relating Reynolds stresses to the mean velocity

$$-\rho\overline{u_i' u_j'} = \mu_\mathrm{t}\left(\frac{\partial u_i}{\partial x_j} + \frac{\partial u_j}{\partial x_i}\right) - \frac{2}{3}\rho k \delta_{ij} \tag{3}$$

where μ_t is the turbulent viscosity and δ_{ij} Kronecker delta. The most frequently used and relatively simple turbulence model is the k-ε model [5], in which

$$\mu_\mathrm{t} = c_\mu \rho \frac{k^2}{\varepsilon} \tag{4}$$

where k is the turbulent kinetic energy and ε is its dissipation rate obtained from the following equations

$$\rho\frac{\partial k}{\partial t} + \rho u_j \frac{\partial k}{\partial x_j} = \frac{\partial}{\partial x_j}\left[\left(\mu + \frac{\mu_\mathrm{t}}{\sigma_k}\right)\frac{\partial k}{\partial x_i}\right] + G_k - \rho\varepsilon \tag{5}$$

and

$$\rho\frac{\partial \varepsilon}{\partial t} + \rho u_j \frac{\partial \varepsilon}{\partial x_j} = \\ = \frac{\partial}{\partial x_j}\left[\left(\mu + \frac{\mu_\mathrm{t}}{\sigma_k}\right)\frac{\partial \varepsilon}{\partial x_i}\right] + c_{1\varepsilon}\frac{\varepsilon}{k}G_k - c_{2\varepsilon}\rho\frac{\varepsilon^2}{k} \tag{6}$$

Here, G_k represents the generation of turbulent kinetic energy due to the mean velocity gradients

$$G_k = -\rho\overline{u_i' u_j'}\frac{\partial u_j}{\partial x_i} \tag{7}$$

To evaluate G_k in a manner of the Boussinesq hypothesis

$$G_k = \mu_\mathrm{t} S^2 \quad S \equiv \sqrt{2 S_{ij} S_{ij}} \quad S_{ij} = \frac{1}{2}\left(\frac{\partial u_i}{\partial x_j} + \frac{\partial u_j}{\partial x_i}\right) \tag{8}$$

where S is the modulus of the mean rate-of-strain tensor S_{ij}. The model constants c_μ, $c_{1\varepsilon}$, $c_{2\varepsilon}$, and σ_k and σ_ε (turbulent Prandtl numbers for k and ε) have the following default values

$$c_\mu = 0.09 \quad c_{1\varepsilon} = 1.44 \quad c_{2\varepsilon} = 1.92 \\ \sigma_k = 1.0 \quad \sigma_\varepsilon = 1.3 \tag{9}$$

Modelling of the roughness of the terrain is achieved by the well known log-law velocity profile [3, 6]. The atmospheric boundary layer is, in nearly all cases, a turbulent flow over aerodynamically rough surface. Under these conditions, the engineering "law of the wall" is given by [7]

$$\frac{u}{u^*} = \frac{1}{\kappa}\ln\frac{z}{z_0} + B \tag{10}$$

where $\kappa = 0.40$ and $B = 5.5$ are used for a smooth terrain (dependent on the roughness height z_0), u^* is the friction velocity, and u the kinematic viscosity.

Governing Equations for the Contaminant Transport

Dispersion of gases in the atmosphere typically occurs through the movement of the mean fluid flow, and diffusion, which is caused by the effect of turbulent fluctuations of the fluid flow, and molecular diffusion, which is negligible in turbulent flows. According to the law of mass conservation the mass balance equation of a contaminant is defined by the equation

$$\rho\frac{\partial w}{\partial t} + \rho u_j \frac{\partial w}{\partial x_j} = \rho\frac{\partial}{\partial x_j}\left[(D + D_\mathrm{t})\frac{\partial w}{\partial x_i}\right] \tag{11}$$

where w is the mass fraction of contaminant, D the molecular diffusion coefficient, and D_t the turbulent diffusion coefficient which can be evaluated by the equation

$$D_\mathrm{t} = \frac{\mu_\mathrm{t}}{\rho Sc_\mathrm{t}} \tag{12}$$

where Sc_t is the turbulent Schmidt number. Sc_t has been taken to be a constant value, namely 0.7, *e.g.* in [8]. However, this value is correct only in the case of fluid flow where the momentum transport is nearly as intense as the mass transfer. It is clear that the momentum transport and the mass transfer are not constant and they are changing through the boundary layer. *Koeltzsch* [9] showed that the turbulent Schmidt number depends strongly on the height within the boundary layer. This work was focused on the experimental study of the atmospheric boundary layer (also other boundary layers) in wind tunnels and the variation of the turbulent Schmidt number, Sc_t, with the height in the boundary layer z/δ was demonstrated. This dependence is depicted in Fig. 1 in form of a

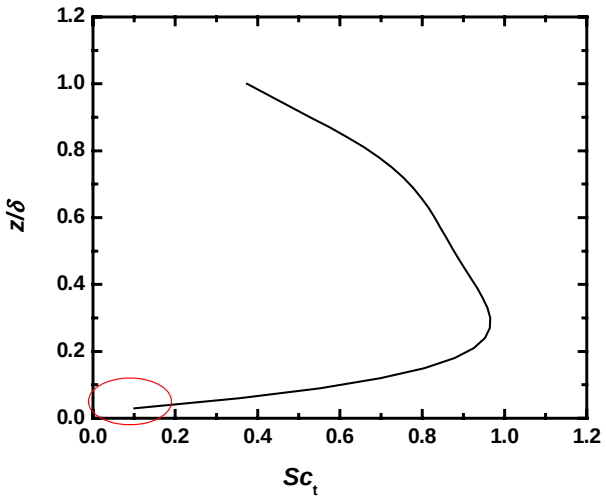

Fig. 1. Variation of the turbulent Schmidt number with the height in boundary layer, eqn (*13*).

polynomial curve (*13*) derived from the experimental results.

$$Sc_\mathrm{t} = \sum_{i=0}^{5} a_i \, (z/\delta)^i$$
$$a = (-0.226, 12.2, -46.2, 81.0, -67.9, 21.5) \quad (13)$$

It is generally accepted that the height of the atmospheric boundary layer is between 600—1000 m and the CFD modelling of gas dispersion is done for the layer height of 10—50 m. Then, $z/\delta \approx 0.05$ and Sc_t should not exceed the value of 0.1 as shown by the circle in Fig. 1. *Raupach et al.* [10] found that near the wall the lower values of the Schmidt number are probably caused by sweeps. Sweeps are coherent structures, which transport fresh air from the upper area of the boundary layer into the region close to the ground, providing it with a high momentum. These sweeps are more intensive in the case of atmospheric stability classes A (highly unstable or convective). Stability is a term used qualitatively for the property of the atmosphere, which governs the accelerations of the vertical motion of air. The acceleration is positive in an unstable atmosphere (turbulence increases), zero when the atmosphere is neutral, and negative (deceleration) when the atmosphere is stable (turbulence is suppressed). Using eqn (*11*) it can be shown that for the turbulent mass transport the following formulation is valid

$$\overline{u'_z C'} = D_\mathrm{t} \frac{\mathrm{d}C}{\mathrm{d}z} \quad (14)$$

where u'_z is fluctuation of the velocity component normal to the ground. This means that the turbulent diffusion coefficient should be correlated with the momentum flux and also the momentum flux decrease with an increase of atmospheric stability. Furthermore, it is evident that the momentum flux increases with the decrease of atmospheric stability and therefore the turbulent Schmidt number also reflects the atmospheric stability.

On the other hand, the momentum flux determines the lateral effect on the value of the vertical entrainment velocity into the plume, u_e, which is a function of the ambient friction velocity (a function of the effect of the surface roughness length), u^*, and the plume Richardson number, Ri^*. The plume Ri^* can be defined by the following equation

$$Ri^* = \frac{g(\rho_\mathrm{p} - \rho_\mathrm{a})h}{\rho_\mathrm{a} u^{*2}} \quad (15)$$

where h is the local plume depth, ρ_p the local plume density, and ρ_a the ambient air density. *Hanna* and *Steinberg* [11] stated for Ri^* values up to 20 the following relation

$$u_\mathrm{e}/u^* = 0.65/(1.0 + 0.2\,Ri^*) \quad (16)$$

From eqns (*15*), (*16*) it follows that with increasing u^* Ri^* decreases and the ratio u_e/u^* increases and *vice versa*. If the value of vertical entrainment velocity significantly increases, *e.g.* due to the high value of momentum sweeps, the plume Ri^* decreases, which means that the plume is more intensively diluted.

Experimental Data and Boundary Conditions

Experiments [2] were carried out for a small release of chlorine (about 0.5 kg min^{-1}). Gaseous chlorine was released during 4.5 min at 30 cm above the ground level. The chlorine concentration in air was measured by UV spectrophotometry. The lowest detectable value was 11 ppm, therefore, contents lower than 11 ppm were approximated to zero. Sensors were distributed at 10 m, 20 m, and 30 m from the release point for Trial 1 and Trial 2 and in the distance of 5 m, 10 m, and 15 m from the source for Trial 3. Experimental data were compared with those modelled by CFD. Table 1 gives the meteorological conditions

Table 1. Experimental Data of Chlorine Release [1]

Parameter	Trial 1	Trial 2	Trial 3
Release rate/(kg min^{-1})	0.54	0.45	0.33
Wind speed/(m s^{-1})	1.1	0.5	1.7
Temperature/ ℃	25	26	26
Relative humidity/%	30	30	30
Solar radiation/(W m^{-2})	715	760	570
Distance from the source/m	Measured content/ppm		
5	–	–	488
10	18	93	54
15	–	–	17
20	12	16	–
30	<11	<11	–

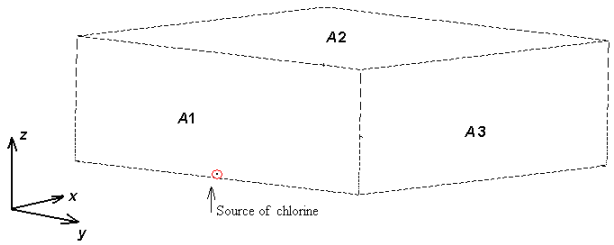

Fig. 2. Geometrical model used in CFD modelling.

and measured concentrations for the three trials done in this experiment.

The geometrical model used to describe the experiment was a 3D block of the size 30 m × 30 m × 10 m (Fig. 2). This block was meshed using tetrahedral elements, with a line mesh of 40, 40, and 20 in the x, y, and z coordinate directions with mesh refining close to the source of chlorine (small circle in Fig. 2). According to Table 1 the stability category for modelling was identified as stability category A, *i.e.* unstable conditions. Thus, the input velocity and its profile [12] (assuming rural conditions of the land [13]) is defined on the area $A1$ as

$$u = u_{10}\left(\frac{z}{10}\right)^{m} \qquad m = 0.07 \qquad (17)$$

where 10 is the height in meters above the ground with corresponding wind velocity u_{10} in this height. Prior to applying eqn (*11*) for calculation of species transport, kinetic energy and dissipation of kinetic energy profiles corresponding to the evolved fluid flow were used.

On the area parallel to $A1$ an outflow boundary condition is assumed, *i.e.* the outflow relative pressure is zero. On the area $A2$, its parallel area, and area $A3$ a symmetry boundary condition is used. On the area parallel to $A3$ (ground) the wall boundary condition was applied. Source strength of chlorine was set according to each trial.

RESULTS AND DISCUSSION

The influence of the turbulent Schmidt number on modelled concentration profile for the atmospheric stability class A and chlorine release corresponding to experimental data for Trial 1 is illustrated in Fig. 3. It is evident that Sc_t significantly influences the chlorine concentration profile. According to eqns (*11*)—(*14*) the turbulent Schmidt number decrease causes an increase of the turbulent diffusion coefficient due to intensive vertical motion by sweeps. Then, from eqn (*16*) it follows that the chlorine plume is more diluted and chlorine is intensively dispersed in both, vertical and horizontal, directions.

Fig. 4 depicts the chlorine concentration at the centreline for the different Sc_t values. It seems that the centreline concentration decreases significantly with the decreasing value of the turbulent Schmidt number. Therefore, for accurate CFD simulation of ground level contaminant concentrations the appropriate Sc_t should be derived from experimental data.

Tables 2—4 summarize results of experiments, CFD modelling, and also results computed by ALOHA (Aerial Locations of Hazardous Atmospheres, computer program developed by the Environmental Protection Agency in the USA), for the three trials performed. The best approximation of experimental data was obtained by CFD modelling using $Sc_t = 0.01$. These results are in a good agreement with experimental observations shown in Fig. 1. For $Sc_t \approx 0.7$ CFD modelling overestimates the chlorine concentration getting values similar to those obtained by ALOHA.

Direct comparisons of the predicted and measured concentrations show that although the predicted concentrations are of the correct order of magnitude, the shapes of the concentration *vs.* distance curves differ from those measured. This indicates that other factors are also important, such as z_0, or the differences

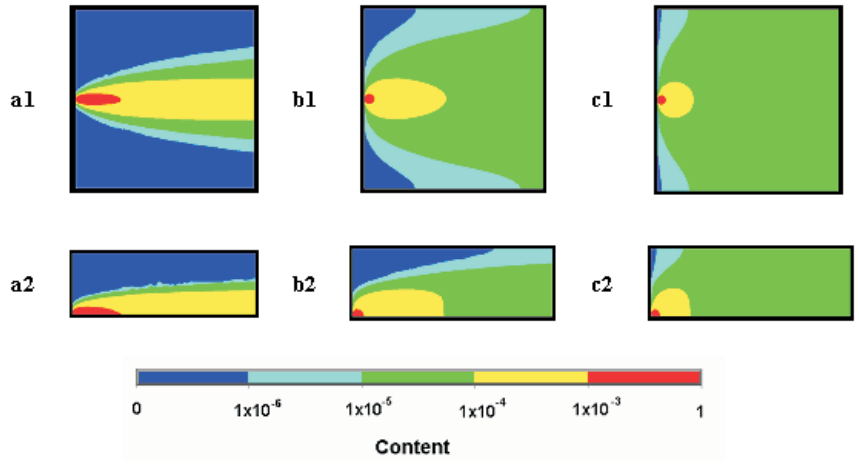

Fig. 3. CFD calculated concentration profiles for $z_0 = 0.1$ m. View from the top, 30 cm above the ground (1), and from the side of centreline (2): *a*) $Sc_t = 0.001$; *b*) $Sc_t = 0.01$; *c*) $Sc_t = 0.1$.

Table 2. Comparison between Measured and Computed Cl_2 Concentrations for Trial 1

Downwind distance	Content/ppm					
m	Measured	ALOHA	CFD Modelling			
			$Sc_t = 0.001$	$Sc_t = 0.01$	$Sc_t = 0.1$	$Sc_t = 0.3$
10	18	43700	58	130	708	1670
20	12	384	37	75	349	805
30	<11	151	34	55	240	519

Table 3. Comparison between Measured and Computed Cl_2 Concentrations for Trial 2

Downwind distance	Content/ppm					
m	Measured	ALOHA	CFD Modelling			
			$Sc_t = 0.001$	$Sc_t = 0.01$	$Sc_t = 0.1$	$Sc_t = 0.3$
10	93	45500	53	142	981	2360
20	16	342	36	75	464	1120
30	<11	141	33	54	310	710

Table 4. Comparison between Measured and Computed Cl_2 Concentrations for Trial 3

Downwind distance	Content/ppm					
m	Measured	ALOHA	CFD Modelling			
			$Sc_t = 0.001$	$Sc_t = 0.01$	$Sc_t = 0.1$	$Sc_t = 0.3$
5	488	233000	134	302	1980	4490
10	54	54000	64	149	887	1990
15	17	27000	50	106	571	1290

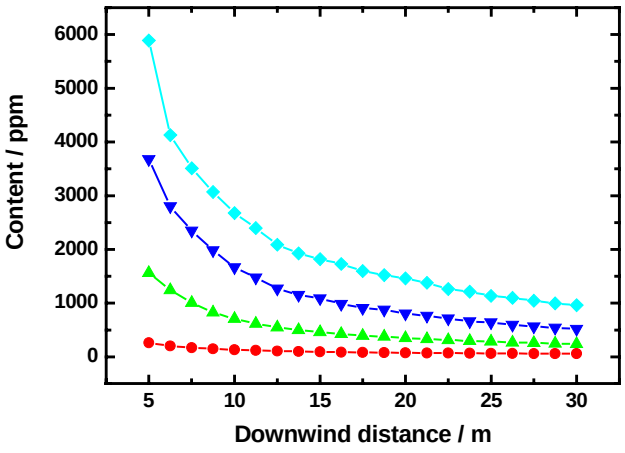

Fig. 4. Centreline concentration profile calculated for roughness $z_0 = 0.1$ m and different turbulent Schmidt number: $Sc_t = 0.01$ (●), $Sc_t = 0.1$ (▲), $Sc_t = 0.3$ (▼), and $Sc_t = 0.7$ (◆).

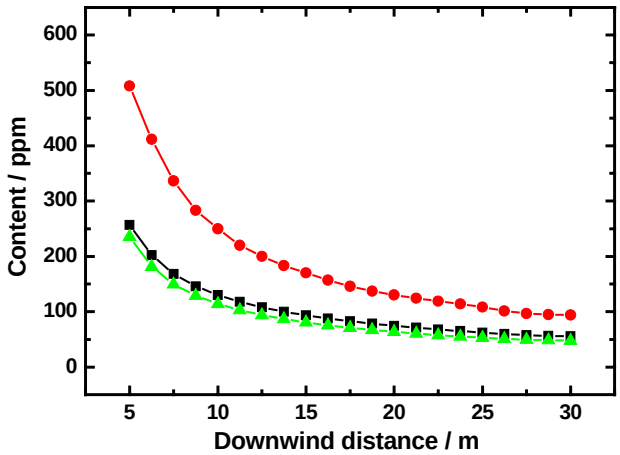

Fig. 5. Centreline concentration profile calculated for $Sc_t = 0.01$ and different roughness heights: $z_0 = 0.5$ m (▲), $z_0 = 0.1$ m (■), and $z_0 = 0.0$ m (●).

between the vertical and horizontal dispersion coefficients.

Transport and dispersion in the atmospheric boundary layer are strongly influenced by the friction velocity, u^*, which is also a function of the surface roughness length, z_0. From eqn (*16*) it follows that the vertical entrainment rate is directly proportional to u^*, *i.e.* the increasing of the surface roughness length, z_0, increases also the dispersion of the released gas plume. Fig. 5 shows the dependence of the centreline chlorine concentration obtained from CFD modelling on the surface roughness length, z_0. One can observe

that by increasing the roughness length the mean contaminant concentration decreases, which is in good agreement with the theory mentioned above.

Acknowledgements. This project was financed by the Slovak Scientific Grant Agency VEGA, Grant No. 1/1377/04.

REFERENCES

1. Lees, F. P., *Loss Prevention in the Process Industries, Hazard Identification, Assessment and Control*, 2nd Edition, Vol. *3*. Butterworth—Heineman, Oxford, 1996.
2. Dandrieux, A., Dusserre, G., and Ollivier, J., *J. Loss Prevention in the Process Industries 15*, 5 (2002).
3. Pope, S. B., *Turbulent Flows*. Cambridge University Press, Cambridge, 2000.
4. Hinze, J. O., *Turbulence*. McGraw-Hill, New York, 1975.
5. Launder, B. E. and Spalding, D. B., *Comput. Methods Appl. Mechanics Eng. 3*, 269 (1974).
6. White, F. M., *Viscous Fluid Flow*. McGraw-Hill, New York, 1991.
7. Hanna, S. R. and Britter, R. E., *Wind Flow and Vapor Cloud Dispersion at Industrial and Urban Sites*. AIChE, New York, 2002.
8. Riddle, A., Carruthers, D., Sharpe, A., McHugh, C., and Stocker, J., *Atmos. Environ. 38*, 1029 (2004).
9. Koeltzsch, K., *Atmos. Environ. 34*, 1147 (2000).
10. Raupach, M. R., Finnigan, J. J., and Brunet, Y., *Boundary-Layer Meteorology 78*, 351 (1996).
11. Hanna, S. R. and Steinberg, K. W., *Atmos. Environ. 35*, 2223 (2001).
12. Mohan, M. and Siddiqui, T. A., *Atmos. Environ. 32*, 3775 (1998).
13. Crowl, D. A. and Louvar, J. F., *Chemical Process Safety: Fundamentals with Applications*. Prentice-Hall, Englewood Cliffs, NJ, 1990.